
VOLUME 114
ISSUE 5
17 MAY 2010
ELSEVIER
Remote Sensing of Environment
http://www.elsevier.com/locate/rse

Remote Sensing of Environment 114 (2010) 1002–1007

Contents lists available at ScienceDirect

Remote Sensing of Environment

journal homepage: www.elsevier.com/locate/rse

Satellite and surface-based remote sensing of Saharan dust aerosols

Sundar A. Christopher [a,b,*], Thomas A. Jones [b]

[a] Department of Atmospheric Science, The University of Alabama in Huntsville, 320 Sparkman Dr., Huntsville AL, United States
[b] Earth System Science Center, The University of Alabama in Huntsville, 320 Sparkman Dr., Huntsville AL, United States

A R T I C L E I N F O

Article history:
Received 26 October 2009
Received in revised form 6 December 2009
Accepted 12 December 2009

Keywords:
Aerosols
Dust
Remote sensing
AERONET
Forcing
MODIS
CERES

A B S T R A C T

The spatial and temporal characteristics of dust aerosols and their properties are assessed from satellite and ground-based sensors. The spatial distribution of total column aerosol optical depth at 550 nm (AOD) from the Moderate Resolution Imaging SpectroRadiometer (MODIS) coupled with top of atmosphere Clouds and the Earth's Radiant Energy System (CERES) shortwave fluxes are examined from the Terra satellite over the Atlantic Ocean. These data are then compared with AOD from two Aerosol Robotic Network (AERONET) ground-based sun photometer measurement sites for nearly six years (2000–2005). These two sites include Capo Verde (CV) (16°N, 24°W) near the Saharan dust source region and La Paguera (LP) (18°N, 67°W) that is downwind of the dust source regions. The AOD is two to three times higher during spring and summer months over CV when compared to LP and the surrounding regions. For a unit AOD value, the *instantaneous* TOA shortwave direct radiative effect (DRE) defined as the change in shortwave flux between clear and aerosol skies for CV and LP are −53 and −68 Wm^{-2} respectively. DRE for LP is likely more negative due to fall out of larger particles during transport from CV to LP. However, separating the CERES-derived DRE by MODIS aerosol effective radii was difficult. Satellite and ground-based dust aerosol data sets continue to be useful to understand dust processes related to the surface and the atmosphere.

1. Introduction

The Sahara is the largest source of windblown dust aerosols (Prospero et al., 2002) and accounts for nearly 50% of dust supplied to the oceans (Miller et al., 2004). During the April–October months over the Saharan desert, northeasterly trade winds have sufficient wind speeds to dislodge sediments from the ground to the atmosphere (Koren & Kaufman, 2004). While the Bodele (~17°N, 18°E) in Chad is the largest source of dust aerosols in the Sahara, other sources in Western Africa include areas in Mali, Mauritania, and Algeria (Goudie & Middleton, 2001). However, the source strength of dust aerosols has been difficult to estimate with values ranging from 100–1500 million tons per year. Nearly 240 Tg of dust is transported annually into and across the Atlantic Ocean (Kaufman et al., 2005) with 50 Tg fertilizing the Amazon basin (Koren et al., 2006) alone. Transport from the Sahara to the Caribbean takes approximately 5–7 days and varies seasonally (Prospero & Carlson, 1981). The main component of Saharan dust is silica (~60%) with varying concentrations of Al_2O_2, Fe_2O_3, CaO, MgO, and K_2O (Goudie & Middleton, 2001; Chudnovsky et al., 2009). Particle sizes near the source regions are larger while downwind in the Caribbean, particle sizes are smaller due to fallout of larger particles during their transport over the Atlantic Ocean (Prospero et al., 2002). The effective radii of dust aerosols can range from 0.1 µm to 10 µm (Tegen & Lacis, 1996) depending upon various factors including proximity to source, physical, chemical and dynamical processes. Over the Saharan Desert and into the eastern North Atlantic, dust aerosols can reach upwards of 5 km above the surface allowing for both long-range transport and significant radiative effects to occur (Christopher et al., 2009; Kaufman et al., 2005).

Dust aerosols from the Saharan Desert have a wide range of impacts from impairing visibility, affecting health, serving as nutrient source for oceans, affecting algal blooms, modifying rainfall, affecting storm activities, reducing surface temperatures and affecting regional climate (see Goudie & Middleton, 2001 for a review). Dust aerosols are studied largely from ground measurements at strategic locations that provide hourly information of dust concentrations and particle sizes (Holben et al., 1998). Concerted field experiments involving aircraft measurements coupled with ground and satellite data sets have proved invaluable for studying dust in the Atlantic (e.g. Reid et al., 2003; Tanré et al., 2003). However, satellite remote sensing provides a cost effective alternative for obtaining spatial distribution of aerosols and their properties although *most* satellite measurements provide very little information on the vertical structure of aerosols. More recently, an active two channel, polarization lidar known as Cloud Aerosol Lidar with Orthogonal Polarization (CALIOP) on the CALIPSO satellite was launched to obtain the vertical structure of clouds and aerosols, although its limited spatial sampling prevents daily global coverage (see Christopher et al., 2009 for a multi satellite-sensor case study on dust aerosols).

* Corresponding author. Department of Atmospheric Science, The University of Alabama in Huntsville, 320 Sparkman Dr., Huntsville AL, United States. Tel.: +1 256 961 7872.
E-mail address: sundar@nsstc.uah.edu (S.A. Christopher).

0034-4257/$ – see front matter © 2010 Elsevier Inc. All rights reserved.
doi:10.1016/j.rse.2009.12.007

The last decade has seen a surge in satellite remote sensing of dust aerosols, not only qualitatively, but also quantitatively (e.g. Christopher et al., 2009). Satellite measurements from polar orbiting and geostationary instruments such as the Moderate Resolution Imaging SpectroRadiometer (MODIS), Multi-angle Imaging SpectroRadiomter (MISR), Clouds and the Earth's Radiant Energy System (CERES) scanner, Ozone Monitoring Instrument (OMI), Polarization and Directionality of the Earth's Radiances (POLDER), CALIOP, Spinning Enhanced Visible and Infrared Imager (SEVIRI), and Atmospheric Infrared Sounder (AIRS) are all providing observations of dust aerosols from regional to global scales (see Forster et al., 2007 for a list of all satellites and their capabilities). These measurements are now being used to validate numerical models and are also being used in data assimilation to improve forecasts of dust aerosols and their impacts (e.g. Greed et al., 2008).

In this paper we first show various satellite imagery and products along with ground-based data to assess instantaneous, hourly, daily, seasonal and yearly distributions and properties form the Saharan Desert and into the Atlantic Ocean. We further quantify the Aerosol Optical Depth at 550 nm (AOD) and associated properties at two locations, including Capo Verde (CV) near the source and another downwind at La Paguera (LP). Finally, we assess the TOA shortwave direct radiative effects at these locations using satellite-based aerosol and shortwave fluxes to determine if the changes in dust aerosol characteristics as they travel westward produce a measurable effect to DRE. Satellite remote sensing alone can provide reliable information on dust aerosols at large spatial scales as described in this paper. They are an invaluable tool for validating numerical models and for studying dust transport pathways from Africa to the Americas.

2. Data and methods

We use the Aerosol Robotic Network (AERONET) data at Capo Verde (CV — 16°N, 24°W) and La Paguera (LP — 18°N, 67°W) along with the Terra–MODIS AOD from March 2000 to December 2005. AERONET is a network of sunphotometers that provides AOD at seven wavelengths and properties such as aerosol size and absorption/scattering characteristics. These well calibrated measurements are available from several hundred worldwide locations (Holben et al., 1998).

MODIS level 1B radiances are used to show an example of reflected solar radiation of clouds and aerosols and we superimpose the level 2 retrieved AOD from both the operational Collection 5 AOD (Levy et al., 2007; Remer & Kaufman, 2006) coupled with the Deep Blue AOD over bright targets (Hsu et al., 2006). The Collection AODs are available over dark targets such as oceans and vegetated areas and the retrieved AODs are within 20% of the AERONET AODs at 550 nm (Levy et al., 2007; Remer & Kaufman, 2006). The Deep Blue AOD product is relatively new and continues to undergo revisions but preliminary comparisons also show that the Deep Blue AODs are within 20% of the AERONET (Hsu et al., 2006). We show the multi-year mean spatial distribution of AODs over the Atlantic Ocean and we also assess the aerosol transport using NCEP winds at 850 hPa.

To assess the instantaneous top of atmosphere shortwave radiative fluxes between clear and aerosol sky regions, we use broadband (0.2–4.5 μm) shortwave fluxes from the Clouds and the Earth's Radiant Energy System (CERES) scanners on Terra and Aqua. The well calibrated CERES radiances are converted to fluxes using empirical Angular Dependence Models (ADMs) (Zhang et al., 2005). The current CERES-SSF product does not contain empirical ADMs as a function of sun-satellite viewing geometry, AOD, and aerosol size. Using the Tropical Rainfall Measuring Mission (TRMM) data for the tropics, and a radiative transfer models these ADMs are constructed by assuming that all aerosols are pure scatterers. Using Terra data, Zhang et al. (2005) constructed a complete set of ADMs using MODIS AOD and particle size information over the global oceans. The differences in TOA fluxes between the CERES-SSF ADMs and those developed by Zhang et al. (2005) are larger than 10 Wm^{-2} per unit AOD. The difference between the CERES clear and aerosol pixels at the TOA is called the

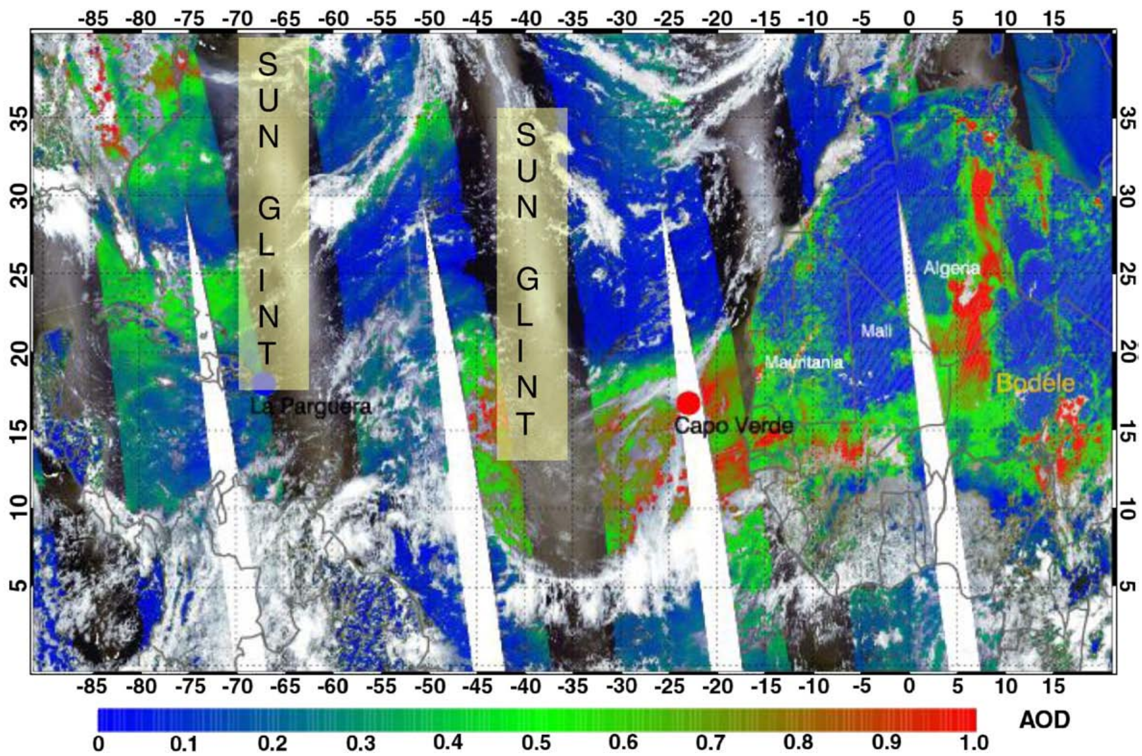

Fig. 1. MODIS level 1B 550 nm radiances with MODIS level 2 aerosol optical depth (AOD) overlaid for the Saharan Desert and the North Atlantic Ocean from the Terra satellite on June 18, 2007. The white strips are missing data due to orbital gaps. Also seen are sunglint areas where no MODIS AOD retrievals are performed. Clouds are shown in white and aerosols optical depth at 550 nm is shown in various colors ranging from blue to red indicating low to high concentrations.

Direct Radiative Effect (DRE), which provides a quantitative assessment of how aerosols change the TOA fluxes. The clear sky fluxes are estimated for 1°×1° regions over the oceans by regressing the AOT versus the shortwave flux. The shortwave flux extrapolated to zero AOT is the clear sky flux. See Zhang et al. (2005) for further details.

3. Results and discussions

To gain a sense of the information available from satellite-based sensors, we combine MODIS level 1B visible radiances (1 km) with level 2 AOD products (10 km) for an example of a large Saharan dust outbreak that occurred on June 18, 2007 (Fig. 1). Using red, green, and blue channel radiances, highly reflective clouds can be seen in white whereas the ocean background has a dark blue appearance. A band of clouds south of 10°N shows clouds and downdrafts from these clouds are often thought to transport dust from the surface into the atmosphere (Goudie & Middleton, 2001). Just north of the cloud region, a large dust plume is evident running from the African coast and into the central Atlantic. Overlaid on the radiance data are the MODIS Collection 5 AODs from the operational algorithm, with color scale

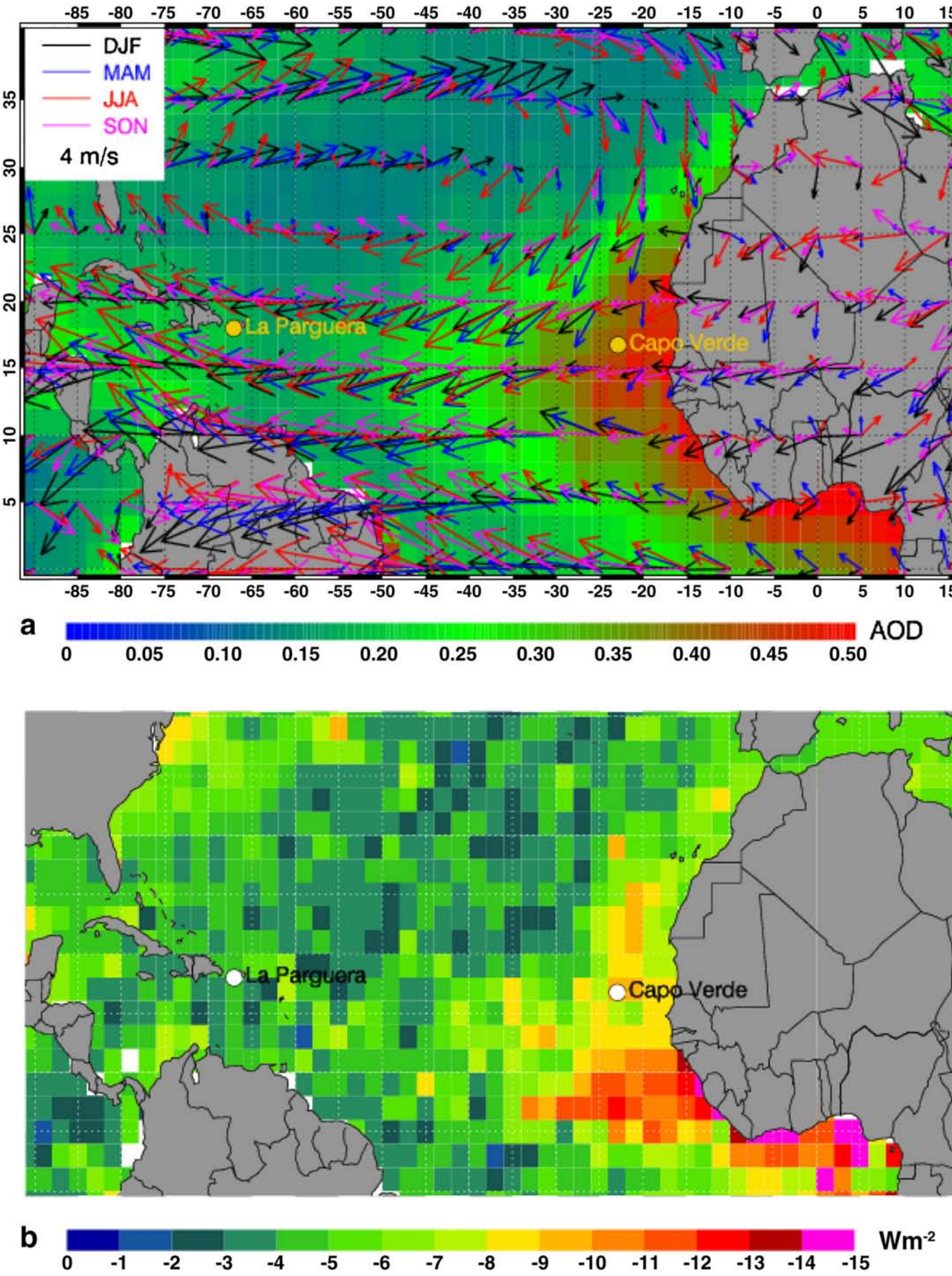

Fig. 2. (a) Annually averaged Terra-MODIS AOT at 500 nm for the North Atlantic Ocean. High AOD values associated with dust are evident along the west coast of Africa and gradually decrease as dust is transported westward by the prevailing wind, which is shown by the wind vectors with the length of the line in the legend representing a wind speed of 4 ms^{-1}. NCEP winds at 850 hPa were averaged over each season (DFJ—black, MAM—blue, JJA—red, SON—pink) and plotted to show mean dust transport characteristics. (b) Diurnally averaged SWRE for the same region where negative values indicating SW cooling due to aerosols.

from blue to red corresponding from low to high AODs. These AODs are retrieved over cloud-free ocean and dark surface areas (south of 10°N). The Deep Blue AODs are superimposed over bright targets (i.e. Saharan Desert). High dust AOD can be seen over source regions such as the Bodele (17°N, 18°E), over Mauritania, and Mali. High AODs values are also seen in the Atlantic Ocean for this day that affects visibility and regional radiative energy budgets. Dust plumes over these desert regions can be as high as 5–6 km above the surface (e.g. Christopher et al., 2009).

To assess the spatial distribution of dust over the Atlantic we provide a 6-year mean Terra-MODIS AOD distribution in Fig. 2. The NCEP 850 hPa winds at 2.5° resolution averaged for each season are shown in various colors. Also shown are the location of the AERONET sites at CV and LP. High AOD values are evident in a latitudinal band from 0 to 25°N (Fig. 2a). Not all of these aerosols are dust since biomass-burning activities frequently occurs in the sub-Sahel area producing smoke that is also transported westward into the Atlantic. During most of the year, the North Atlantic between 20–30°N is dominated by high pressure with winds rotating clockwise around the location of highest pressure. South of 25°N wind is generally from the east transporting the dust and biomass-burning aerosols westward into the Atlantic. The greatest westward transport occurs during the summer months (JJA) when pressure gradients and wind speeds are greatest. Dust is transported southwest from the Saharan Desert into the eastern Atlantic near CV and then further westward into the Atlantic until it reaches the Caribbean and LP. Note that north of 25°N the winds are westerly bringing pollution from the eastern United States into the Atlantic although these AODs are much smaller and are not transported beyond 50–55°W. Diurnally averaged annual SWRE over the north Atlantic is greatest west of the African coast with values between -6 and $-8\ \mathrm{Wm^{-2}}$ around Capo Verde. SWRE in excess of $-10\ \mathrm{Wm^{-2}}$ is present further south where AOT is also high (>0.5) and dust may become mixed with smoke from biomass burning (Fig. 2b). SWRE generally decreases further to the west as AOD decreases. Around La Parguera, SWRE is approximately $-4\ \mathrm{Wm^{-2}}$, over 50% smaller than at Capo Verde corresponding to a similar decrease in AOT (Fig. 2a).

The summer season is dominated by dust aerosols originating from the Sahara and reaching the Caribbean, southern Africa, and the continental United States. High AOD values above 0.5 near the coast of Africa are reduced to about half of that value in LP largely due to the fallout of larger dust aerosol particles (Reid et al., 2003). To assess the magnitudes of AODs at CV and LP from the MODIS and the AERONET, we show the 550 nm monthly-mean AODs in Fig. 3 from March 2000 to December 2005. Fig. 3a and b clearly shows the spring–summer maxima over both CV and LP. The monthly-mean AODs at LP shows a single broad spring–summer peak whereas at CV there appears to be two broad peaks, one during the spring–summer season and the other during winter. Since CV is closer to the Saharan dust sources, the changes in dust concentrations from different Saharan dust sources

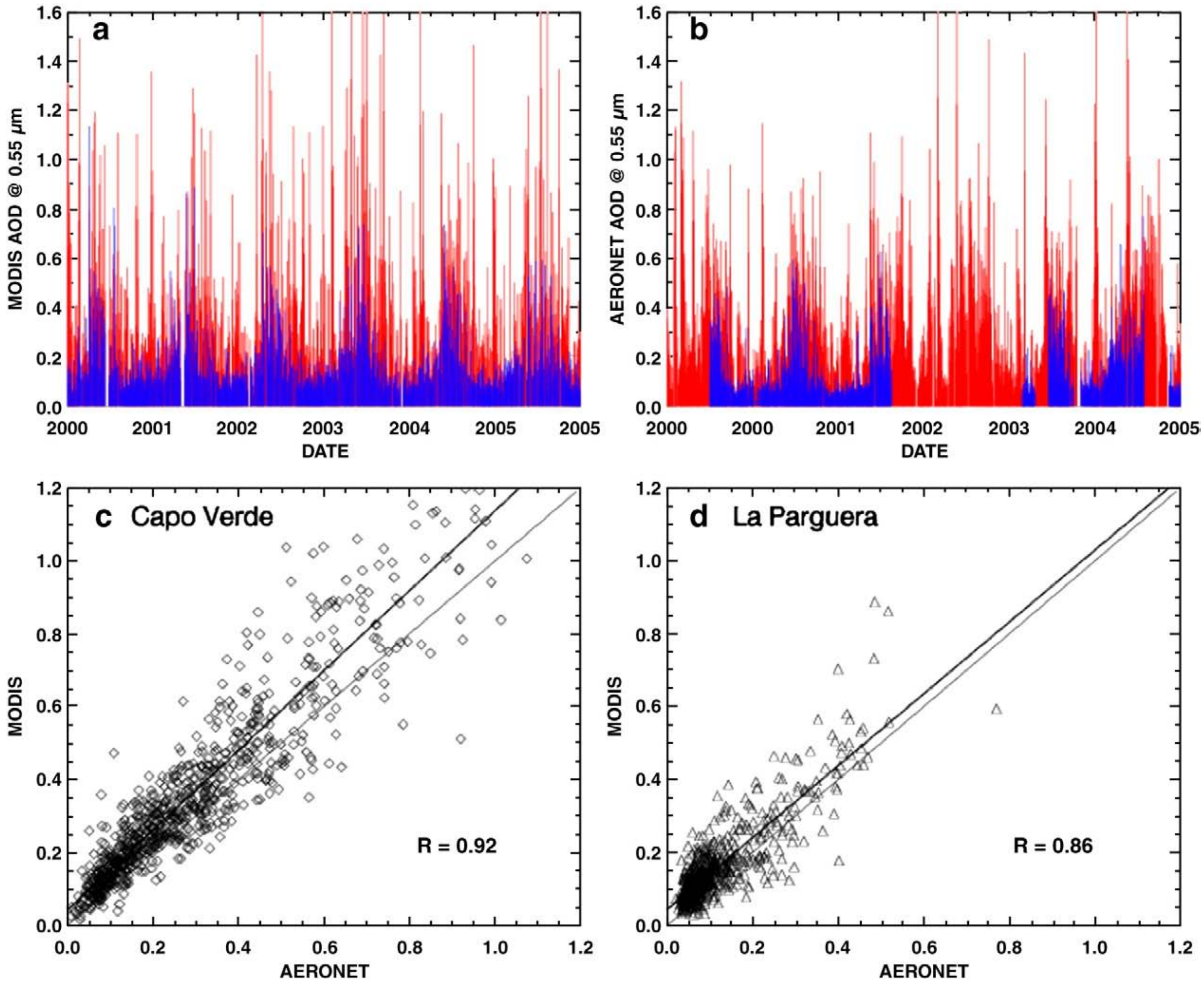

Fig. 3. Mid-visible AOD at 550 nm over Capo Verde (CV, red) and La Paguera (LP, blue) between March 2000 and December 2005, from a) MODIS, and b) AERONET. Corresponding scatter plots of MODIS AOT as a function of AERONET AOT are shown in panels c (Capo Verde) and d (La Paguera). Note that AOD is greatest during the summer months at both sites associated with the increase in dust aerosols and that AOD is always greater at CV, since it is much closer to the dust source regions.

are seen in CV as well. For example, while the Bodele is a significant source of dust aerosols throughout the year, the largest dust concentrations over Bodele are during the winter season (Prospero et al., 2002). Fig. 3c and d shows the relationship between MODIS and AERONET AODs for CV and LP respectively. The satellite-derived AODs are well correlated with AERONET values although at CV there is a larger scatter at higher AODs.

To assess the particle size properties from MODIS, we show the aerosol effective radii retrievals over CV and LP. The aerosol effective radius is the ratio of the third to the second moment of the size distribution and is derived from look up table-based retrieval that contains four fine modes and five coarse mode aerosols. The MODIS aerosol effective radii are within 25% of the AERONET-derived values (Remer et al., 2005). The particle sizes at CV are larger since they are closer to the source region compared to aerosols near LP since larger dust particles fall out of the atmosphere during the westward transport of dust across the Atlantic Ocean (Fig. 4). The frequency of smaller particles is higher in LP when compared to CV although both large and small particles exist in both locations. The spatial distribution of both the SW and LW radiative effects has also been demonstrated (Christopher & Jones, 2007) and therefore we only assess the CERES TOA shortwave DRE as a function of effective radii at CV and LP only for this discussion. Fig. 5 shows the DRE for aerosols as a function of MODIS AOD for CV (Fig. 5a) and LP (Fig. 5b) respectively. The range of AODs at CV is much larger than those at LP. The slope of DRE/AOD called the *instantaneous* radiative efficiency is more negative for LP (-68 Wm^{-2}/AOD) when compared to LP (-53 Wm^{-2}/AOD). The diurnally averaged values in this region are approximately half of the instantaneous values. It is tempting to conclude that since LP has smaller particles that provide a larger surface area the reflectivity is higher and therefore the efficiencies are more negative. However, based on this data set alone we cannot make that conclusion since AODs at LP do not reach beyond 0.6 although from Fig. 5b we can see that there are dominated by smaller size effective radii values. Nevertheless using multiple data sets such as AERONET, MODIS, and CERES, we can confirm that the MODIS AOD and CERES fluxes are well correlated with larger AODs in CV when compared to LP.

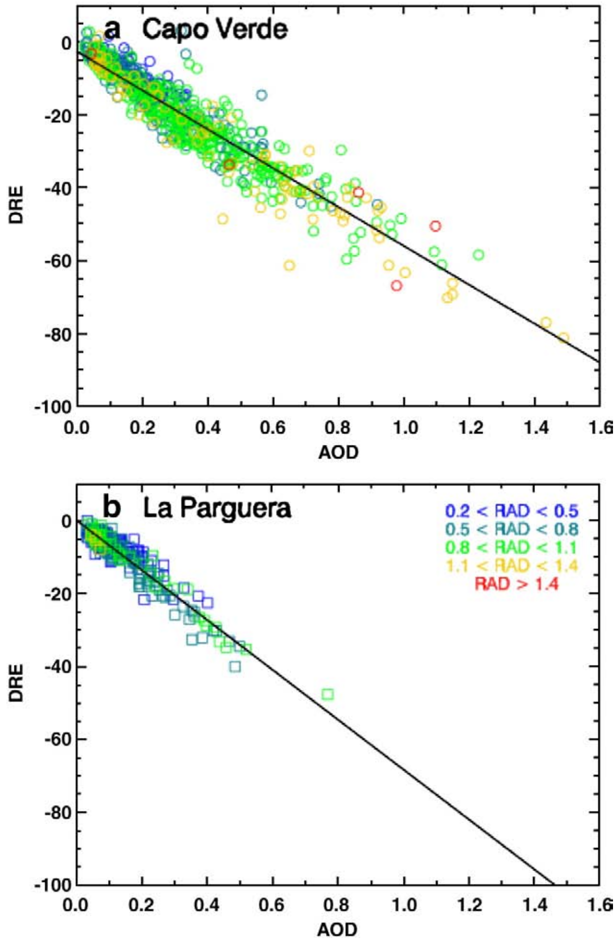

Fig. 5. Shortwave aerosol radiative effect (DRE, Wm^{-2}) as a function of MODIS AOT for Capo Verde (a) and La Paguera (b) binned by aerosol effective radius (RAD). For both regions, the relationship is nearly linear, but higher AODs and larger dust particles are primarily located at Capo Verde.

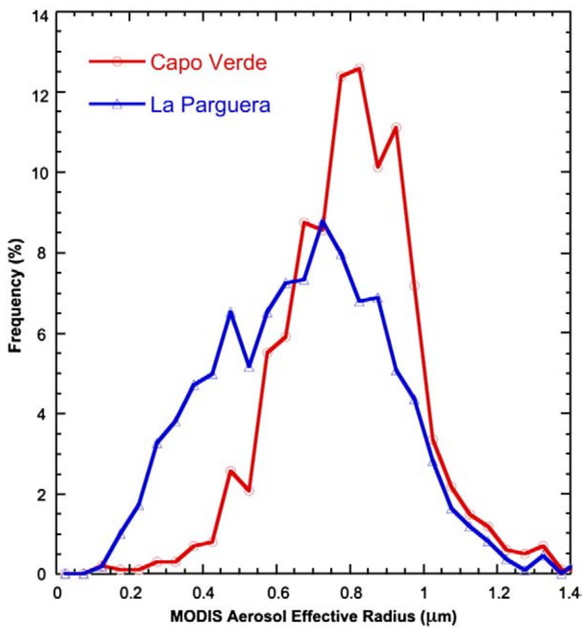

Fig. 4. Frequency distribution of MODIS aerosol effective radius (μm) at both Capo Verde and La Paguera. The important point is the larger aerosols are more likely to be present at Capo Verde, since the larger dust aerosol particles will fall out of the atmosphere during their transport westward.

4. Summary and conclusions

Nearly a ten-year record of aerosol data from Terra is now available on a near global basis. These data are being used to assess several applications including climate and air quality. In this paper, we assess the spatial distribution of aerosols using the Terra-MODIS over a six year period coupled with an assessment of aerosol properties from two sun photometers — one near the dust source and another far downwind. Our major conclusions are as follows, the AOD at CV is two to three times larger than at LP with broad spring–summer maxima; the *instantaneous* DRE per unit optical depth over CV is less negative (-53 Wm^{-2}) than LP (-68 Wm^{-2}) suggesting that smaller particles may be responsible for the increased reflectivity; MODIS aerosol effective radii at LP are smaller than at CV since larger particles rapidly fall out during the westward transport of dust.

Acknowledgements

This research is supported by NASA's Radiation sciences, Interdisciplinary sciences, an EOS grant, and ACMAP programs. The data were obtained through the NASA Langley Distributed Active Archive Systems and other data sets.

References

Christopher, S. A., Johnson, B., Jones, T. A., & Haywood, J. (2009). Vertical and spatial distribution of dust from aircraft and satellite measurements during the GERBILS field campaign. *Geophysical Research Letters*, *36*, L06806. doi:10.1029/2008GL037033.

Christopher, S. A., & Jones, T. (2007). Satellite-based assessment of cloud-free net radiative effect of dust aerosols over the Atlantic Ocean. *Geophysical Research Letters*, *34*, L02810. doi:10.1029/2006GL027783.

Chudnovsky, A., Ben-Dor, E., Kostinski, A. B., & Koren, I. (2009). Mineral content analysis of atmospheric dust using hyperspectral information from space. *Geophysical Research Letters*, *36*, L15811. doi:10.1029/2009GL037922.

Forster, P., Artaxo, P., Berntsen, T., Betts, R., Fahey, D. W., Haywood, J., et al. (2007). Changes in atmospheric constituents and in radiative forcing. *Climate Change 2007: The Physical Science BasisContribution of Working Group I to the Forth Assessment Report of the Intergovernmental Panel on Climate Change*. Cambridge: Cambridge University Press.

Goudie, A. S., & Middleton, M. J. (2001). Saharan dust storms, nature and consequences. *Earth-Science Reviews*, *56*, 179—204.

Greed, G., Haywood, J. M., Milton, S., Keil, A., Christopher, S., Gupta, P., et al. (2008). Aerosol optical depths over North Africa: 2. Modeling and model validation. *Journal of Geophysical Research*, *113*, D00C05. doi:10.1029/2007JD009457.

Holben, B. N., Eck, T. F., Slutsker, I., Tanre, D., Buis, J. P., Setzer, A., et al. (1998). AERONET — A federated instrument network and data archive for aerosol characterization. *Remote Sensing of Environment*, *66*(1), 1—16.

Hsu, N. C., Tsay, S. -C., King, M. D., & Herman, J. R. (2006). Deep blue retrievals of Asian aerosol properties during ACE-Asia. *IEEE Transactions on Geoscience and Remote Sensing*, *44*, 3180—3195. doi:10.1109/TGRS.2006.879540.

Kaufman, Y. J., Koren, I., Remer, L. A., Tanre´, D., Ginoux, P., & Fan, S. (2005). Dust transport and deposition observed from the Terra-Moderate Resolution Imaging Spectroradiometer (MODIS) spacecraft over the Atlantic Ocean. *Journal of Geophysical Research*, D10S12. doi:10.1029/2003JD004436.

Koren, I., & Kaufman, Y. J. (2004). Direct wind measurements of Saharan dust events from Terra and Aqua satellites. *Geophysical Research Letters*, *31*, L06122. doi:10.1029/2003GL019338.

Koren, I., Kaufman, Y. J., Washington, R., Todd, M. C., Rudich, Y., Martins, J. V., et al. (2006). The Bodélé depression: A single spot in the Sahara that provides most of the mineral dust to the Amazon forest. *Environmental Research Letters*, *1*, 014005. doi:10.1088/1748-9326/1/1/014005 (5 pp.).

Levy, R. C., Remer, L. A., Mattoo, S., Vermote, E. F., & Kaufman, Y. J. (2007). Second-generation operational algorithm: Retrieval of aerosol properties over land from inversion of Moderate Resolution Imaging Spectroradiometer spectral reflectance. *Journal of Geophysical Research*, *112*, D13211. doi:10.1029/2006JD007811.

Miller, R. L., Tegen, I., & Perlwitz, J. (2004). Surface radiative forcing by soil dust aerosols and the hydrologic cycle. *Journal of Geophysical Research*, *109*, D04203. doi:10.1029/2003JD004085.

Prospero, J., & Carlson, T. N. (1981). Saharan outbreaks over the tropical North Atlantic. *Pure and Applied Geophysics*, *119*, 677—691.

Prospero, J. M., Ginoux, P., Torres, O., Nicholson, S., & Gill, T. (2002). Environmental characterization of global sources of atmospheric soil dust derived from the Nimbus 7 Total Ozone Mapping Spectrometer (TOMS) absorbing aerosol product. *Reviews of Geophysics*, *40*(1), 1002. doi:10.1029/ 2000RG000095.

Reid, J. S., Kinney, J. E., Westphal, D. L, Holben, B. N., Welton, E. J., Tsay, S. -C., et al. (2003). Analysis of measurements of Saharan dust by airborne and ground-based remote sensing methods during the Puerto Rico Dust Experiment (PRIDE). *Journal of Geophysical Research*, *108*(D19), 8586. doi:10.1029/2002JD002493.

Remer, L. A., & Kaufman, Y. J. (2006). Aerosol direct radiative effect at the top of the atmosphere over cloud free ocean derived from four years of MODIS data. *Atmospheric Chemistry and Physics*, *6*(237–20), 253.

Remer, L. A., Kaufman, Y. J., Tanré, D., Mattoo, S., Chu, D. A., Martins, J. V., et al. (2005). The MODIS aerosol algorithm, products and validation. *Journal of Atmospheric Science*, *62*, 947—973.

Tanré, D., Haywood, J., Pelon, J., Léon, J. F., Chatenet, B., Formenti, P., et al. (2003). Measurement and modeling of the Saharan dust radiative impact: Overview of the Saharan Dust Experiment (SHADE). *Journal of Geophysical Research*, *108*(D18), 8574. doi:10.1029/2002JD003273.

Tegen, I., & Lacis, A. (1996). Modeling of particle size distribution and its influence on the radiative properties of mineral dust aerosol. *Journal of Geophysical Research*, *101*, 19237—19244.

Zhang, J., Christopher, S. A., Remer, L. A., & Kaufman, Y. J. (2005). Shortwave aerosol cloud-free radiative forcing from Terra, I: Angular models for aerosols. *Journal of Geophysical Research-Atmospheres*, *D10*, S23. doi:10.1029/2004jd005008.